PROCEEDINGS
OF THE
NATIONAL ACADEMY OF SCIENCES
Volume 30 March 15, 1944 Number 3
Copyright 1944 by the National Academy of Sciences

RESPIRATORY RATES OF THE SHOOT TIPS AND MATURING TISSUES IN LUPINUS ALBUS AND TROPAEOLUM MAJUS

By Ernest Ball* and Edgar J. Boell

Osborn Botanical Laboratory and Osborn Zoölogical Laboratory, Yale University

Communicated February 3, 1944

It has long been recognized that the shoot apex in the higher plants serves as the region from which new tissues of the primary plant body are produced.[1–9] Indeed, Bower[2] has characterized the activities of this meristem as an indefinitely continued embryology.

The work of several authors[12–15] suggests that the shoot apex may influence, to some extent at least, the differentiative activity of subjacent tissues in the plant, for when shoot apices are regenerated in mature parenchymatous tissues, the new shoot apices apparently induce the formation of vascular strands which connect with the original conductive system of the shoot. In somewhat the same way the so-called organizers in the animal embryo have been demonstrated to influence the development and differentiation of other regions. Accordingly it would be of interest to determine whether the metabolic characteristics of the organizer[19] and of the plant shoot apex are to some extent similar.

Furthermore, in view of the widely current idea, originally enunciated by Pfeffer,[16] that growth is usually accompanied by elevated respiratory activity, it is especially important to study the relationship between respiration and growth in the shoot apex. The embryonic region exhibits the highest growth rate of the shoot on the basis of the following criteria of growth—frequency of cell division, synthesis of protoplasm, and changes in shape and structure associated with the production of foliar primordia—and if Pfeffer's thesis is correct, it therefore ought to possess the greatest respiratory activity.

Some experimental work has previously been done on the respiration of various gross regions along the developing plant axis. Thus Kidd, West and Briggs[10] found the liberation of carbon dioxide in the sunflower to be greater in the bud than in more basal tissues. Caldwell and Meiklejohn[11] measured the respiration of the entire terminal bud and of the subjacent

tissues in the tomato and found a gradient of decreasing oxygen consumption from apex to base. However, in order to gain an idea of the significance of respiratory rate in the phenomena of induction, production of foliar primordia and maturation, as well as in the very rapid growth of the shoot apex, still more precise techniques must be applied to very small volumes of tissues. It is necessary to measure separately and with great accuracy the oxygen consumption of the shoot apex (i.e., of the embryonic zone) and of the subjacent regions in which cellular maturation is occurring.

In the present work a comparative survey has been made of the rate of oxygen consumption of the meristematic and of the immediately subjacent maturing tissues in the terminal part of the plant axis, in order to determine the relationship between the respiratory activity of a given region and the degree of its cellular maturation, or its position in the gradient of differentiation.

Materials and Methods.—Young plants of *Lupinus albus* L. and of *Tropaeolum majus* L. were used. *Lupinus* shows strong apical dominance, and branching by the growth of axillary buds is rare. *Tropaeolum*, on the other hand, exhibits apical dominance only during the early seedling stages, and the growth of shoots from all axillary buds soon leads to a much branched condition. Thus, the present work was done upon plants of two different physiological types.

Pieces of tissues, designated as *A*, *B* and *C* in the order of their position down the shoot (Figs. 1 (*a*) and 2 (*a*)) and each having a volume of about 430 μ^3 (ca. 0.08 mm.^{3}), were excised from the shoot tip under the high power of a binocular dissecting microscope equipped with a calibrated ocular. The *A* piece comprised the shoot apex and the three youngest visible foliar primordia. In addition, a small amount of non-apical tissue was also unavoidably included, but since the volume of the latter was insignificant in comparison with that of the apical tissue proper, the oxygen consumption of the *A* piece, for all practical purposes, can legitimately be considered typical of the actual apical tissue. Piece *B* was composed of maturing tissue immediately basal to the *A* piece, while piece *C* represented still further maturing tissue subjacent to region *B*.

The oxygen consumption of the tissues was determined by means of the Cartesian diver technique.[17, 18] Each of the pieces of tissue was placed in the bulb of a diver with 1.5 μl. of Pfeffer's culture solution (Robbins[20]), and readings of oxygen consumption were begun, and continued for periods of four to five hours. During the experiments, the apparatus was darkened in order to prevent photosynthesis in the chlorenchymatous tissues of *Lupinus*.

Results and Discussion.—The results of typical experiments on *Lupinus* and *Tropaeolum* are shown in figures 1 (*b*) and 2 (*b*). The graphs indicate

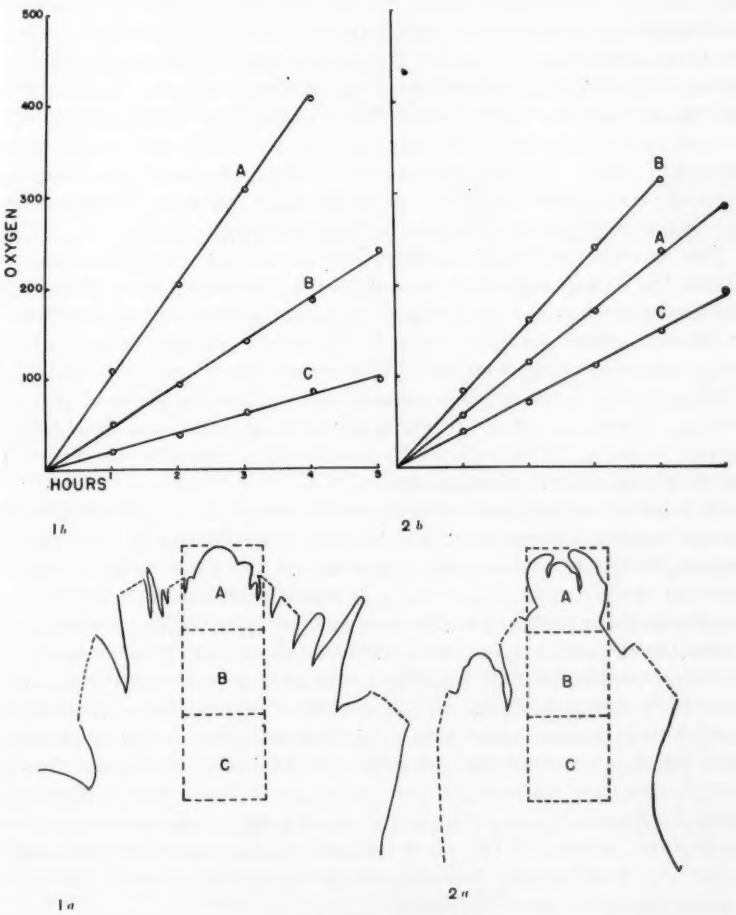

FIGURES 1 AND 2

Figures 1 (*a*) and 2 (*a*) are line drawings of median sections of stem tips of *Lupinus albus* and of *Tropaeolum majus*, respectively, and show the amounts and locations of the *A*, *B* and *C* pieces of tissues.

Figures 1 (*b*) and 2 (*b*) show the oxygen consumption of the *A*, *B* and *C* pieces of tissues in the Cartesian divers. Ordinates denote mμl. of O_2 consumed per piece of tissue (ca. 0.08 mm.^{4}), and abscissas indicate length of time pieces of tissue were in the divers.

Figure 1 (*b*) indicates that there is a decreasing respiratory gradient along the shoot of *Lupinus*. Figure 2 (*b*) indicates that the subjacent (*B*) tissues in the shoot of *Tropaeolum* consumed more oxygen than the shoot tip.

that the rate of oxygen consumption of the excised tissues is essentially uniform during the period of measurement. It is significant that in none of the experiments was there any appreciable acceleration or depression of respiration during the initial phase of the experimental period, because this fact shows that the tissues were neither perceptibly stimulated nor depressed by the processes of excision from the plant body and immersion in the culture fluid. The general linearity of the curves, moreover, attests to the fact that nutritive conditions in the medium were such as to maintain the tissues in an essentially normal physiological state.

The curves reveal significant differences in the rate of oxygen consumption in the various regions of the same plant. Moreover, they show that the respiratory rate of a given region in relation to other regions is different in the two species studied. Thus, in *Lupinus*, a gradient in the rate of respiration decreasing from tip to base seems clearly indicated, while in *Tropaeolum* this is not the case, the most apical portion of the shoot tip (*A*) having a lower rate than the region of maturing cells immediately subjacent. However, in both plants the most basal portion of the shoot tip (*C*) shows the lowest rate of respiration.

Histological examination of the shoot tips of *Lupinus* and of *Tropaeolum* reveals marked differences in the amount of protoplasm in the regions selected for study. Many cells (especially in the shoot apex) of the *A* piece are densely cytoplasmic; those in region *B* are characterized by the beginning of conspicuous vacuolization and the appearance of intercellular spaces, and those in region *C* show still more prominently these indications of cellular maturation. It is highly probable, therefore, that the amount of actively metabolizing material in the three regions is not identical in spite of their volume equivalence. But that the differences in respiration reported above are not due altogether to differences in the amount of actively respiring material per unit of volume is shown by the fact that when respiratory rate is calculated on a dry weight basis the ratio of the respiratory activity in the three regions remains essentially the same (table 1). Fundamental differences in the respiratory rates of the three regions thus seem clearly indicated.

The quantitative differences in the dry weights of the *A*, *B* and *C* pieces, shown in table 1, are reflected also in preliminary data on the total nitrogen content of these regions. Although, as the table reveals, the distribution of total nitrogen does not altogether parallel the dry weight, the respiratory rates when calculated on the basis of total nitrogen show, in general, the same fundamental differences among the regions, and between the two plants.

In *Lupinus*, the respiratory rate of the shoot tip is higher than that of the subjacent tissues while in *Tropaeolum* this appears not to be true. In both *Lupinus* and *Tropaeolum* the shoot apex serves as the region from

which new foliar primordia and new stem tissues are produced, and in both plants, moreover, the apical region displays the highest growth rate of the shoot. It is evident therefore, in view of the data presented, that these activities of the shoot apex are not necessarily correlated with a high respiratory rate. A comparable situation is seen in amphibian develop-

TABLE 1

REGION	NO. OF EXPERIMENTS	MμL. O_2 CONSUMED PER HOUR PER PIECE OF TISSUE (AVERAGE)	μG. DRY WEIGHT PER PIECE (AVERAGE)	MμL. O_2 CONSUMED PER HOUR PER μG. DRY WT. (AVERAGE)	μG. N PER PIECE (AVERAGE)	MμL. O_2 CONSUMED PER HOUR PER μG. OF NITROGEN (AVERAGE)
			Lupinus			
A	11	96	11.0	8.7	0.8	120
B	11	41	9.1	4.5	0.32	128
C	11	22	8.8	2.5	0.45	49
			Tropaeolum			
A	7	57	12.3	4.6	0.89	64
B	7	79	10.5	7.5	0.91	87
C	7	38	8.2	4.7	0.70	55

ment where it appears that the organizer activities of the dorsal lip of the blastopore are not correlated with respiratory level.[19] It may be of some significance that the respiratory activity of the various zones of *Lupinus*, in which apical dominance is manifest, is different from that in *Tropaeolum* where apical dominance is absent.

Summary.—Using the Cartesian diver technique, a study has been made of the respiratory activity in the shoot tips and subjacent tissues of *Lupinus albus* and *Tropaeolum majus*. The results indicate that differences in the distribution of respiratory activity along the apical-basal axis of the shoot exist in the two plants, but that there is apparently no correlation between the developmental activities of a given region and the magnitude of its respiratory rate.

* National Research Council Fellow in Botany, 1941–1942. Present address: Biological Laboratories, Harvard University.

[1] Wolff, C. F., *Theoria generationis*, Halae, 1759.
[2] Bower, F. O., *Botany of the Living Plant*, London, 1919.
[3] Child, C. M., *Jour. Exp. Zool.*, **11**, 187–220 (1911).
[4] Child, C. M., *Individuality in Organisms*, Chicago, 1915.
[5] Child, C. M., *Biol. Bull.*, **39**, 147–187 (1920).
[6] Child, C. M., *Protoplasma*, **5**, 447–476 (1928).
[7] Child, C. M., *Patterns and Problems of Development*, Chicago, 1941.
[8] Foster, A. S., *Bull. Torrey Bot. Club*, **68**, 339–350 (1941).
[9] Thoday, D., *Nature*, **144** (3648), 571–575 (1939).
[10] Kidd, F., West, C., and Briggs, G. E., *Proc. Roy. Soc. Lond.* (*B*), **92**, 368–384 (1921).
[11] Caldwell, J., and Meiklejohn, J., *Ann. Bot.*, N. S., **1**, 477–486 (1937).
[12] Simon, S., *Jahrb. wiss. Bot.*, **45**, 351–478 (1908).
[13] Hammond, B. L., *Bot. Gaz.*, **97**, 834–845 (1936).
[14] Naylor, E. E., and Johnson, B., *Amer. Jour. Bot.*, **24**, 637–678 (1937).

[15] McVeigh, I., *Ibid.*, **25**, 7–11 (1938).
[16] Pfeffer, W., *The Physiology of Plants*, Trans. by A. J. Ewart, Oxford, 1903.
[17] Boell, E. J., and Needham, J., *Proc. Roy. Soc. Lond.* (*B*), **127**, 363–373 (1939).
[18] Boell, E. J., and Woodruff, L. L., *Jour. Exp. Zool.*, **87**, 385–402 (1941).
[19] Boell, E. J., *Growth*, Supplement to Vol. 6, pp. 37–53 (1942).
[20] Robbins, W. J., *Amer. Jour. Bot.*, **29**, 241–245 (1942).

*INVALIDATION OF THE CYTOLOGICAL EVIDENCE FOR RECIPROCAL CHIASMATA IN THE SEX CHROMOSOME BIVALENT OF MALE DROSOPHILA**

BY KENNETH W. COOPER

DEPARTMENT OF BIOLOGY, PRINCETON UNIVERSITY

Communicated February 7, 1944

Darlington's (1934)[1] interpretation of meiosis in male *Drosophila pseudoobscura* involves a mechanical dualism in the modes of conjunction of autosomes and sex chromosomes. Thus autosomes are held to conjoin as bivalents by exaggeration of the forces normally expressed in somatic pairing,[2] whereas sex chromosomes are believed to conjoin solely by chiasmata. The primary evidence which led Darlington to this interpretation is purely cytological, and the more critical points may be resumeed as follows.

(1) Autosomal bivalents have homologues paired throughout their lengths at late diakinesis, *neither contacts* nor chiasmata being visible between them.

(2) In contrast to the autosomal bivalents, from diakinesis to onset of anaphase the sex chromosomes are *in contact* over a short segment of their lengths, and manifestly this is not the whole of their homologous regions. Furthermore, lengths of sex chromosomes which are not conjoined lie part in spite of their homology (Figs. 12 (*d–f*), diakinesis; Figs. 12 (*g–i*), metaphase-I).

(3) At prometaphase and metaphase there appears to be a state of tension between the kinetochores and the points of association in the sex chromosomes (Figs. 12 (*g–i*)).

(4) *X* and *Y* are unchanged when they separate at anaphase (Figs. 12 (*j–k*)). Were a single exchange present between the interstitial segments of contact and conjunction, the morphology of the separating chromosomes would clearly disclose it because *X* and *Y* are heteromorphic.

The striking contrast of the sex chromosome bivalent with the chiasma-free autosomal bivalents led Darlington to suspect that fundamentally different mechanisms are in operation in the two instances. According to

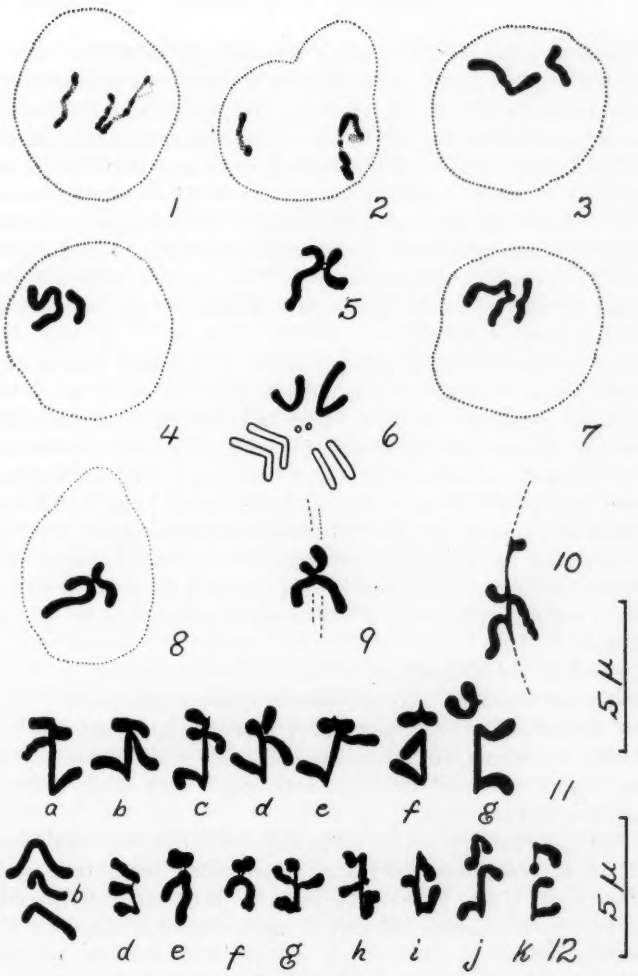

FIGURES 1–12

Comparison of sex chromosome conjunction in the spermatogenesis of *Olfersia bisulcata* Macq. and of *Drosophila pseudoobscura* Frolova. Except for figure 6, only sex chromosomes are illustrated; figures semidiagrammatic.

Figure 1, late diplotene. Figures 2–4, 7, early diakinesis. Figure 5, late diakinesis or early prometaphase. Figure 6, metaphase plate of male gonial cell (sex chromosomes black). Figure 8, late diakinesis. Figures 9, 10, prometaphase. Figures 11 (*a–g*), sex chromosome bivalent of *Olfersia* at metaphase-I (*a–e*) and early anaphase-I (*f*, *g*). Figures 12 (*a–k*), sex chromosomes of *Drosophila pseudoobscura*, redrawn from Darlington (1934).[1] Figure 12 (*a*), the *X*-chromosome. Figure 12 (*b*), *Y*-chromosome of weak-A race. Figure 12 (*c*), *Y*-chromosome of weak-B race. Figure 12 (*d–f*), diakinesis, weak-A race. Figures 12 (*g–i*) metaphase-I, weak-A races. Figures 12 (*j*, *k*) anaphase-I, weak-B races.

Upper scale, approximate magnification for figures of *Olfersia*. Lower scale, approximate magnification for figures of *Drosophila*.

his chiasma hypothesis of metaphase pairing[3] chiasmata provide the primary if not only means of conjunction of the chromosomes as bivalents. Observations (2), (3) and (4) above are compatible with the known properties of bivalents having chiasmata. Darlington[1] thus regards them as affording a demonstration of the presence of chiasmata in the sex chromosome bivalent. Since *genetic* crossing-over between the sex chromosomes of the male of *Drosophila* is rare and probably not a meiotic occurrence, the hypothesized chiasmata must be considered localized in inert regions and invariably to occur in reciprocal pairs. This, in brief, is the nature of the evidence for the reciprocal chiasmata hypothesis of sex chromosome conjunction in male *Drosophila*.

Short, localized, terminal pairing-segments have been discovered in the fly *Melophagus ovinus*.[4] No chiasmata need be assumed to conjoin *Melophagus'* autosomes in these segments at meiosis in the male; yet the autosomal bivalent configurations and behavior closely parallel those of the sex chromosome bivalent in male *Drosophila*.[5] For this reason it was likewise concluded that there is no cytological need to suppose that reciprocal chiasmata conjoin the sex chromosomes of *Drosophila*. The truth of this conclusion is admirably demonstrated by the details of bivalent formation by the sex chromosomes in the male of the fly *Olfersia bisulcata* Macq., a member of the same family to which *Melophagus* belongs (Hippoboscidae).

The diploid chromosome set of male *Olfersia bisulcata* ($2n = 8$) is remarkably different from that of *Melophagus ovinus* ($2n = 18$). There is a pair of submedian autosomes, a pair of nearly terminal autosomes, a pair of dot-like autosomes, and a heteromorphic pair of submedian sex chromosomes (Fig. 6; compare the sex chromosomes with those of *Drosophila pseudoobscura*, Figs. 12 (*a*, *b*, *c*)).[6]

At late diplotene the sex chromosomes of *Olfersia* may easily be recognized; as in *Melophagus* they are neither paired nor even close to one another (Figs. 1, 2). Henceforth, however, their behavior is unlike that of the sex chromosomes of *Melophagus* which remain unpaired, for *X* and *Y* ultimately conjoin in *Olfersia*. It will be seen that the resulting sex chromosome bivalent is identical with that of male *Drosophila pseudoobscura*.

As diakinesis progresses the sex chromosomes move closer together. During this movement an interstitial segment near the kinetochore in each chromosome becomes juxtaposed and finally closely conjoined (Figs. 3–4, 7–8, 5). At prometaphase the sex chromosome bivalent thus formed orients on the spindle (Fig. 9). During this process the regions between the kinetochores and the points of association may become markedly attenuated and hence appear to be in a state of tension (Fig. 10).[7] At late diakinesis, prometaphase and metaphase, the sex chromosomes of male

Olfersia are in contact only over a short interstitial segment of their lengths, and the lengths of the sex chromosomes which are not thus conjoined lie apart (Figs. 5, 8, 9, 10, 11 (*a–e*) of *Olfersia;* compare with Figs. 12 (*d–i*) of the sex chromosome bivalent of *Drosophila pseudoobscura* at the same stages).[8] Furthermore, the sex chromosomes of *Olfersia* are unchanged when they separate at anaphase (Figs. 11 (*f–g*) of *Olfersia;* compare with Figs. 12 (*j–k*) of *Drosophila pseudoobscura*).[9] Thus the sex chromosome bivalent of male *Olfersia* shows the same morphological attributes as are said to characterize the *X-Y* bivalent of *Drosophila*. But inasmuch as the sex chromosomes of male *Olfersia* conjoin *after* condensation, the resulting bivalent must be devoid of chiasmata.[10] Therefore none of the aforementioned attributes, singly or in combination with each other, can be considered to afford a demonstration of the presence of chiasmata. Accordingly it is concluded that there is no longer a cytological need to suppose the existence of reciprocal (or any other) chiasmata in the inert regions of the sex chromosomes of *Drosophila*. Just as in the cases of the autosomes of *Melophagus* and *Olfersia*, and the sex chromosomes of *Olfersia*, the *X-Y* bivalent of male *Drosophila pseudoobscura* may be supposed to be conjoined by means of localized pairing segments which do not form chiasmata.

It is not known whether the sex chromosomes in *Drosophila pseudoobscura* conjoin after or during their completion of condensation. That in fact they may actually conjoin while condensing is suggested by Darlington's[1] observation that at diakinesis not only are some of the sex chromosome bivalents visibly conjoined, but another configuration of sex chromosomes is also found. In this latter case the sex chromosomes are said to show a clear space between them without any visible connection joining the two chromosomes. Until *Drosophila pseudoobscura* is restudied the exact significance of this fact cannot be judged, but it is not improbable that careful seriation will show that the connected bivalents are a consequence of pairing after or during condensation as has been found to be the case in *Olfersia*. Such delayed pairing following condensation is not unique. There are many instances known of similar chromosomal maneuvers in other insects, some of which Schrader[11] has briefly reviewed. The entire problem of bivalent formation and modes of conjunction requires reanalysis, for the chiasma hypothesis of metaphase pairing is clearly incapable of generalizing all of the facts.

* This work was supported by a grant from the Penrose Fund of the American Philosophical Society, to which organization grateful acknowledgment is made.

[1] Darlington, C. D., *Genetics*, **19**, 95–118 (1934).

[2] This view is implicit in Steven's (*Jour. Exp. Zool.*, **5**, 359–374 (1908)) classic and initial account of spermatogenesis in male flies, and underlies my interpretation of the *Melophagus* case as well. Bauer (*Fortschr. Zool.*, **4**, 584–597 (1939)) and Wolf (*Chromosoma*, **2**, 192–246 (1941)) have questioned the validity of such an interpretation of autosomal conjunction at meiosis. Their arguments will be examined elsewhere.

[3] Darlington, C. D., *Jour. Gen.*, **21**, 17–56 (1929).

[4] Cooper, K. W., *Proc. Nat. Acad. Sci.*, **27**, 109–114 (1941).

[5] The only striking difference is that conjunction is terminal in *Melophagus* and interstitial in the sex chromosomes of *Drosophila*.

[6] Although the meiotic autosomal bivalents of *Olfersia* can be shown to conjoin by conjunctive segments devoid of chiasmata as in *Melophagus*, they will not be discussed here nor be illustrated. Suffice it to say that the bivalent formed by the submedian pair of autosomes is more complicated in structure than earlier believed (Cooper, K. W., *Amer. Phil. Soc. Yearbook, 1941*, pp. 122–127, (1942)), and only in the disjunction figures does it resemble autosomal bivalents of *Drosophila*.

[7] Hence identical with point (3), page 50.

[8] Hence identical with point (2), page 50.

[9] Hence identical with point (4), page 50.

[10] The extensive cytological data which show crossing-over to be a zygotene or pachytene event make implausible the assumption that crossing-over may occur between markedly condensed, post-pachytene chromosomes.

[11] Schrader, F., in: *Cytology, Genetics and Evolution*, University of Pennsylvania Press, Philadelphia, 1941, pp. 27–36.

BIRKHOFF'S THEORY OF GRAVITATION AND EINSTEIN'S THEORY FOR WEAK FIELDS

By Alberto Barajas

Institute of Mathematics, National University of Mexico

Communicated February 9, 1944

Recently, in the widely read *Mathematical Reviews*,[1] Weyl has commented on Birkhoff's theory of gravitation of 1942,[2] suggesting that it is much the same as a limiting form of Einstein's well-known theory of 1916 for weak fields, characterized by Weyl as follows: "If one writes the equations of Einstein's theory of gravitation for g_{ik} differing but infinitely little from the constant values of δ_{ik} characteristics for flat space-time, $g_{ik} = \delta_{ik} + h_{ik}$, and neglects higher powers of h_{ik}, one obtains a theory with a symmetric tensor of gravitation h_{ik} in a flat world, which in its factual consequences agrees almost completely with Einstein's original theory." I propose to show[3] that this degenerate form is fundamentally different from Birkhoff's theory and is unsatisfactory from a physical point of view. In doing so, attention will be limited to gravitational fields in empty space.

Birkhoff's space-time is the same as Minkowski's with $ds^2 = dt^2 - dx^2 - dy^2 - dz^2$. His fundamental gravitational tensor h_{ij} satisfies the equation $\Box h_{ij} = 0$ in empty space, and the equations of motion of a free particle in an arbitrary gravitational field are:

$$\frac{d^2x^i}{ds^2} = \delta^{pi}\left(\frac{\partial h_{jp}}{\partial x^k} - \frac{\partial h_{jk}}{\partial x^p}\right)u^j u^k$$

where $\delta^{pi} = 1$ for $p = i = 1$, $\delta^{pi} = -1$ for $p = i = 2, 3, 4$, zero otherwise, and $u^i = dx^i/ds$.

In the general relativity theory of Einstein the quadratic fundamental form may be written $ds^2 = (\delta_{ij} + H_{ij})dx^i dx^j$. For weak gravitational fields, it is readily shown that H_{ij} may be chosen so that Einstein's gravitational equation $R_{\mu\nu} = 0$ reduces to $\Box H_{ij} = 0$.[4] The equations of motion of a free particle are, for this degenerate case:

$$\frac{d^2x^i}{ds^2} = -g^{pi}\left(\frac{\partial H_{jp}}{\partial x^k} - \frac{1}{2}\frac{\partial H_{jk}}{\partial x^p}\right)u_j u^k$$

In this expression, ds is, of course, the interval in a curved space-time, not Minkowski's ds, although Weyl (loc. cit.) considers the degenerate theory to have reference to "a flat world."

If we consider the static field due to a mass-point m, for reasons of symmetry, H_{ij} must have the form (r = radial distance):

$$H_{ij} = \begin{Vmatrix} a/r & 0 & 0 & 0 \\ 0 & b/r & 0 & 0 \\ 0 & 0 & b/r & 0 \\ 0 & 0 & 0 & b/r \end{Vmatrix}$$

with $a = -2m$ so as to obtain the classical Newtonian result in the first approximation. Let us now compare Birkhoff's and Einstein's theories.

Birkhoff's theory:

Flat space-time: $ds^2 = dt^2 - dx^2 - dy^2 - dz^2$.

Gravitational tensor: $h_{ij} = \begin{Vmatrix} m/r & 0 & 0 & 0 \\ 0 & m/r & 0 & 0 \\ 0 & 0 & m/r & 0 \\ 0 & 0 & 0 & m/r \end{Vmatrix}$ with $\Box h_{ij} = 0$.

Equations of motion of a particle in the plane $z = 0$

$$x'' = -\frac{mx}{r^3} - \frac{2mx}{r^3}(x'^2 + y'^2) + \frac{mx'r'}{r^2},$$

$$y'' = -\frac{my}{r^3} - \frac{2my}{r^3}(x'^2 + y'^2) + \frac{my'r'}{r^2}.$$

Advance of perihelion: $\dfrac{6\pi m}{a(1 - e^2)}$.

Bending of light rays: $\dfrac{4m}{p}$.

Red shift[5] $\Delta\lambda/\lambda$: $\frac{m}{r}$.

Degenerate form of Einstein's theory:

Curved space-time: $ds^2 = (1 - 2m/r)dt^2 - (1 + b/r)(dx^2 + dy^2 + dz^2)$.

Gravitational tensor: $H_{ij} = \begin{Vmatrix} -2m/r & 0 & 0 & 0 \\ 0 & b/r & 0 & 0 \\ 0 & 0 & b/r & 0 \\ 0 & 0 & 0 & b/r \end{Vmatrix}$.

Equations of motion of a particle in the plane $z = 0$

$$x'' \doteq -\frac{mx}{r^3} - \frac{bx'r'}{r^2} - \frac{(m - b/2)x}{r^3}(x'^2 + y'^2),$$

$$y'' \doteq -\frac{my}{r^3} - \frac{by'r'}{r^2} - \frac{(m - b/2)y}{r^3}(x'^2 + y'^2).$$

Advance of perihelion: $\frac{-3b + 2m}{a(1 - e^2)}\pi$.

Bending of light rays: $\frac{2m - b}{p}$.

Red shift $\Delta\lambda/\lambda$: $\frac{m}{r}$.

From this it follows that, in order to obtain the correct advance of the perihelion one must place $b = -4m/3$ and, in order to obtain the correct bending of light, one should place $b = -2m$ which is contradictory.

The red shift is accounted for in Birkhoff's theory as due to the energy loss of the photon while it travels from the emitting body to the earth. On the basis of this alternative interpretation, but using the degenerate form of the equations, b would then have to vanish, $b = 0$, to obtain the correct result.

On the other hand, in the *flat* space-time of the degenerate form of Einstein's theory the atomic clock would register imaginary time at distances less than $2m$ from the mass-point at the origin!

The introduction of the two arbitrary constants a and b is not in keeping with the spirit of Einstein's original theory, one of whose chief advantages is the elimination of arbitrary constants. Besides, if in the energy tensor $T^{ij} = \rho u^i u^j - p g^{ij}$ one sets $p = 0$, in accordance with the fact that the potential pressure energy is small, as Einstein has done, then $b = 0$ necessarily follows.

Another characteristic feature of Birkhoff's theory should be carefully emphasized: the trajectories of free particles are not geodesics in any curved four-dimensional space-time, i.e., no $d\sigma^2 = g_{ij}dx^i dx^j$ exists in which Birkhoff's trajectories are geodesics. In fact for light rays one would have, on the one hand $d\sigma^2 = g_{ij}dx^i dx^j = 0$ and on the other $ds^2 = \delta_{ij}dx^i dx^j = 0$, from which $g_{ij} = k\delta_{ij}$, k = constant, would follow. Otherwise, we may establish our statement thus: the equations of the geodesics in the $d\sigma$-space are:

$$u^p\left(\frac{d^2x^i}{ds^2} + \Gamma^i_{\alpha\beta}u^\alpha u^\beta\right) = u^i\left(\frac{d^2x^p}{ds^2} + \Gamma^p_{\alpha\beta}u^\alpha u^\beta\right)$$

Multiplying by u_i and adding with respect to i one obtains:

$$u^p u^i \Gamma^i_{\alpha\beta}u^\alpha u^\beta = \frac{d^2x^p}{ds^2} + \Gamma^p_{\alpha\beta}\,u^\alpha u^\beta$$

from which we get

$$\frac{d^2x^p}{ds^2} = (u^p u_i \Gamma^i_{\alpha\beta} - \Gamma^p_{\alpha\beta})\,u^\alpha u^\beta.$$

Now the trajectories of free particles in Birkhoff's theory are given by

$$\frac{d^2x^p}{ds^2} = \delta^{\mu p}\left(\frac{\partial h_{\alpha\mu}}{\partial x^\beta} - \frac{\partial h_{\mu\beta}}{\partial x^\mu}\right)u^\alpha u^\beta;$$

therefore one should have identically[6]

$$\delta^{\mu p}\left(\frac{\partial h_{\alpha\mu}}{\partial x^\beta} - \frac{\partial h_{\alpha\beta}}{\partial x^\mu}\right) = u^p u_i\,\Gamma^i_{\alpha\beta} - \Gamma^p_{\alpha\beta}.$$

But the left-hand member of this equation is a function of t, x, y, z, only, while the right-hand member is a function of t, x, y, z, and u^k; therefore the two members cannot be identical unless $\Gamma^i_{\alpha\beta} = 0$ which is a trivial case. This completes our proof.[7]

[1] *Mathematical Reviews*, **4**, 285 (Nov. 1943).

[2] These PROCEEDINGS, **29**, 231 (1943).

[3] During the last two months G. D. Birkhoff, Carlos Graef, Manuel Sandoval Vallarta and I have been collaborating intensively in a study of Birkhoff's theory of gravitation, matter and electricity in flat space-time, and its consequences. The present note owes much to our joint discussions.

[4] See, for instance, R. C. Tolman, *Relativity, Thermodynamics and Cosmology*, Oxford, 1934, p. 236.

[5] Obtained by use of photon as light carrier. All formulas are taken only in the first approximation.

[6] The components of u^i are related by $\delta_{ij}u^i u^j = 1$.

[7] Weyl's other comments will be taken up separately by Manuel Sandoval Vallarta.

ON THE THEORY OF CHARACTERS OF GROUPS AND SEMI-GROUPS IN NORMED VECTOR RINGS

By Einar Hille

Department of Mathematics, Yale University

Communicated February 4, 1944

1. Recently I. Gelfand[1] has defined a class of characters of Abelian groups embedded in a normed commutative vector ring. The present note contains an elaboration of this theory with a strengthening of the main theorem and extensions to semi-groups.

Let $\mathfrak{R}$ be a normed commutative vector ring with unit element e, $\mathfrak{M}$ the set of maximal ideals $\mathfrak{M}$ in $\mathfrak{R}$, $\mathfrak{R}/\mathfrak{M}$ the corresponding residue class rings each of which is a field. Defining the norm $||X||$ of a residue class X, modulo $\mathfrak{M}$, as $\min ||x||$ for $x \in X$, Gelfand shows that $\mathfrak{R}/\mathfrak{M}$ is a normed field and hence isomorphic with the complex field. Let X_α be the class of elements congruent to αe (mod. $\mathfrak{M}$), α arbitrary complex number. Then $\bigcup X_\alpha = \mathfrak{R}$ and $X_\alpha + X_\beta = X_{\alpha+\beta}$, $X_\alpha X_\beta = X_{\alpha\beta}$.

Define[2]

$$\mu(x;\ \mathfrak{M}) = \alpha, \qquad x \equiv \alpha e \ (\text{mod. } \mathfrak{M}). \tag{1}$$

Since $x - \alpha e$ is singular for every $x \in X_\alpha$, the spectrum $\sigma(x)$ of x contains the point $\lambda = \alpha$. Conversely, if $\alpha \in \sigma(x)$, there exists an $\mathfrak{M}$ such that $x \equiv \alpha e$ (mod. $\mathfrak{M}$). Since $|\mu(x;\ \mathfrak{M})| \leq \max |\sigma(x)| \leq ||x||$, $\mu(x;\ \mathfrak{M})$ is a bounded functional which is additive as well as multiplicative

$$\mu(x+y;\ \mathfrak{M}) = \mu(x;\ \mathfrak{M}) + \mu(y;\ \mathfrak{M}), \mu(xy;\ \mathfrak{M}) = \mu(x;\ \mathfrak{M})\mu(y;\ \mathfrak{M}). \tag{2}$$

In particular, $\mu(x;\ \mathfrak{M})$ is continuous.

Finally the notion of quasi-nilpotency will be needed. An element q of $\mathfrak{R}$ is quasi-nilpotent if $e - \alpha q$ has an inverse for every complex α or, which is equivalent in a normed vector ring, if $||q^n||^{1/n} \to 0$ when $n \to \infty$. The quasi-nilpotent elements form an ideal, the radical of $\mathfrak{R}$, which equals the intersection of all maximal ideals.

After these introductory remarks we proceed to the subject matter proper.

2. Let $\mathfrak{G}$ be a set of elements in the ring $\mathfrak{R}$ which form a group under the operation of ring multiplication. For every $\mathfrak{M} \in \mathfrak{M}$ the bounded linear multiplicative functional $\mu(x;\ \mathfrak{M})$ for x in $\mathfrak{G}$ defines a continuous one-dimensional representation $\Gamma(\mathfrak{M})$ of $\mathfrak{G}$, $\mu(x;\ \mathfrak{M})$ being the characters of the representation.

THEOREM 1. *$\Gamma(\mathfrak{M})$ is unitary in the sense that $|\mu(x;\ \mathfrak{M})| = 1$ on $\mathfrak{G}$ for every $\mathfrak{M} \in \mathfrak{M}$ if and only if for all $x \in \mathfrak{G}$*

$$\lim_{n\to\infty} ||x^n||^{1/n} = 1, \qquad \lim_{n\to\infty} ||x^{-n}||^{1/n} = 1. \tag{3}$$

Condition (3) expresses that the spectrum of x lies on the unit-circle. Since $\sigma(x)$ is the range of $\mu(x;\ \mathfrak{M})$ for $\mathfrak{M} \in \mathbf{M}$ and fixed x, this is all that should be proved.

The main question in the representation theory is whether or not there are enough representations available so that any given pair of distinct elements of the group have distinct characters in at least one representation. The limitations of the present theory are clearly brought out by

THEOREM 2. *If $x \neq y$ are two elements of $\mathfrak{G}$, then $\mu(x;\ \mathfrak{M}) = \mu(y;\ \mathfrak{M})$ for all $\mathfrak{M} \in \mathbf{M}$ if and only if $x - y = q$, where q is quasi-nilpotent. This case can arise if and only if $\mathfrak{G}$ contains an element of the form $e + q$ and is excluded if $\mathfrak{R}$ is without radical.*

We omit the proof which is an immediate consequence of the properties of the functional $\mu(x;\ \mathfrak{M})$ listed above.

Gelfand has shown that even if $\mathfrak{R}$ has a radical it is possible to exclude the exceptional elements of the form $e + q$ from the group $\mathfrak{G}$ by requiring that all cyclical subgroups form bounded pointsets in the vector space $\mathfrak{R}$. The following condition is less restrictive.

THEOREM 3. *If $||x^{\pm n}|| = o(n)$ when $n \to \infty$, then x cannot be of the form $e + q$ where q is quasi-nilpotent and $q \neq 0$. The conclusion becomes false if $o(n)$ be replaced by $O(n)$.*

If $x = e + q$ then the resolvent $R(\lambda;\ e + q) = ((\lambda - 1)e - q)^{-1}$ admits of the three expansions

$$\begin{aligned} -(e+q)^{-1} - \textstyle\sum_1^\infty (e+q)^{-n-1}\lambda^n, &\qquad |\lambda| < 1; \\ e\lambda^{-1} + \textstyle\sum_1^\infty (e+q)^n\lambda^{-n-1}, &\qquad |\lambda| > 1; \\ e(\lambda-1)^{-1} + \textstyle\sum_1^\infty q^n(\lambda-1)^{-n-1}, &\qquad \lambda \neq 1. \end{aligned}$$

In the first two series the coefficients are $o(n)$ in norm. A theorem in classical function theory, found by G. Pólya,[3] asserts that if $f(z)$ is an entire function of $w = 1/(z-1)$ and if in the power series expansions of $f(z)$ about 0 and about ∞ the coefficients are $O(n^\nu)$, then $f(z)$ is a polynomial in w of degree $\leq \nu + 1$. If the coefficients are $o(n^\nu)$ instead, the degree will be $< \nu + 1$. By an obvious extension of this theorem to vector valued functions, one concludes that $R(\lambda;\ e + q)$ has a simple pole at $\lambda = 1$ which requires $q = 0$. On the other hand, if q is a nilpotent element such that $q \neq 0$, $q^2 = 0$, then $(e + q)^n = e + nq$ which is $O(n)$ in norm. Thus the stated condition is the best of its kind.

It should be observed that a condition of the form $||x^{\pm n}|| = o(n^m)$, if satisfied by an element of the form $e + q$, requires $q^m = 0$ and this condition is again the best possible.[4]

Combining the preceding theorems we obtain

THEOREM 4. *If the elements of $\mathfrak{G}$ satisfy the condition of Theorem 3, then all representations $\Gamma(\mathfrak{M})$ are unitary and if $x \neq y$, there is a representation in which $\mu(x;\ \mathfrak{M}) \neq \mu(y;\ \mathfrak{M})$.*

3. These considerations may be extended in part to semi-groups. Let $\mathfrak{S}$ be a set of elements in $\mathfrak{R}$ which form a semi-group under ring multiplication so that $x \in \mathfrak{S}$, $y \in \mathfrak{S}$ implies $xy \in \mathfrak{S}$. We shall require that $\mathfrak{S}$ be closed under inversion so that if x is regular and is in $\mathfrak{S}$ then x^{-1} is also in $\mathfrak{S}$.

The functionals $\mu(x;\ \mathfrak{M})$ also provide one-dimensional representations $\Sigma(\mathfrak{M})$ of $\mathfrak{S}$. It is obviously meaningless to require that $\Sigma(\mathfrak{M})$ be unitary. If $x \neq y$ are two elements of $\mathfrak{S}$ we still have $\mu(x;\ \mathfrak{M}) = \mu(y;\ \mathfrak{M})$ for all $\mathfrak{M}$ if and only if $x - y = q$. Thus this case can arise only if $\mathfrak{R}$ has a radical, but when present the situation is much more complicated than in the case of groups. Thus as a rule there is no longer a single exceptional class; every singular element $x \in \mathfrak{S}$ may give rise to a class $\{x + q\}$ the elements of which cannot be separated by the representations. Since the condition of Theorem 3 can be applied to regular elements only, the problem of excluding such singular exceptional classes is a much more difficult one which apparently cannot be handled by the methods of the present note.

[1] Gelfand, I., "Zur Theorie der Charaktere der Abelschen topologischen Gruppen," *Rec. Math.*, N. S., **9** (**51**), 49–50 (1941). For the theory of normed vector rings see Gelfand, "Normierte Ringe," *Ibid.*, 3–24, and Lorch, E. R., "The Theory of Analytic Functions in Normed Abelian Vector Rings," *Trans. Amer. Math. Soc.*, **54**, 414–425 (1943).

[2] This is $x(\mathfrak{M})$ in Gelfand's notation. His $x(\mathfrak{M})$, however, is a function on maximal ideals to complex numbers corresponding to a fixed element x of the ring while $\mu(x;\ \mathfrak{M})$ is a function on the ring to complex numbers corresponding to a fixed maximal ideal.

[3] Pólya, G., "Aufgabe 106," *Jahresbericht D.M.V.*, **40**, *81* (1931). Several solutions are published, *Ibid.*, **42** (1933); that by Szegö, G., pp. *15–16*, is short and self-contained. See also the closely related problem 105: an entire function of order one and minimal type which is $O(n^m)$ on the integers is a polynomial of degree $\leq m$.

[4] Cf. Gelfand, I., "Ideale und primäre Ideale in normierten Ringen," *Rec. Math.*, N. S., **9** (**51**), 41–48 (1941), where similar conclusions are drawn less directly from a deeper theorem due to F. and R. Nevanlinna.

GALACTIC AND EXTRAGALACTIC STUDIES, XVII. REVISION OF THE DISTANCES OF THIRTY HIGH-LATITUDE GLOBULAR CLUSTERS

BY HARLOW SHAPLEY

HARVARD COLLEGE OBSERVATORY

Communicated February 7, 1944

1. The distribution of the photoelectrically-measured color classes for sixteen globular clusters in galactic latitudes higher than thirty degrees is as follows:[1]

Color class	*a*5	*f*4	*f*5	*f*6	*f*7	*f*8	*f*9
Numbers	1	1	1	5	1	6	1

with the mean value *f*6.1 ± 0.8(m. e.). The distribution of integrated spectral types, according to Miss Cannon's classification for ten globular clusters in these same latitudes is:

Spectral class	*A*7	*F*5	*F*8	*G*0	*G*	*G*5
Numbers	1	1	1	1	3	3

The difficulty of classification is such that only the mean value of about *G*0 is significant. For the seven high-latitude globular clusters common to both lists we have the mean values, *f*6.7 and *F*8. The clusters certainly are not redder than would be expected from their mean spectral classes.

The foregoing evidence that there is little or no selective space absorption in high latitude is supported also by the work of Stebbins, Whitford and Huffer on the color excesses for stars and galaxies. The distribution of faint galaxies indicates that also the total photographic absorption in high latitude, if not wholly negligible, is at least manageably small. Even down to latitudes of twenty degrees the total absorption, except in a few special longitudes, is not so heavy but that we can, when computing the distances of globular clusters, estimate the amount of light loss from the abundance of external galaxies in the background.

For the sixty known globular clusters of the galactic system in low latitude, $\beta < \pm 20°$, accurate determinations of the distance will long remain difficult. For them the background of external galaxies is absent, or nearly so, and the total absorption cannot therefore be directly estimated. It is precarious to adopt an absorption correction from the observed color excesses because of the large inherent spread in the integrated colors and the possible variability of the ratio of selective to total absorption throughout the various longitudes. All the photometric methods of measuring either the absolute or the relative distances are therefore not encouraging for clusters in low latitude, even when many

Cepheid variables are present; and the astrometric methods (parallax, motions, diameters) are of low value, either because the distances are too great or because of vagueness in the boundaries of clusters in the rich star fields.

Although occasionally in intermediate latitudes, $\pm 20° > \beta > \pm 10°$, the total absorption in the direction of a globular cluster can be estimated from the number of external galaxies in the surrounding field, we may be at a loss to know how much absorption lies between the cluster and the observer and how much lies beyond the cluster but still within the galactic system. All high-latitude globular clusters, however, lie well beyond whatever absorption there may be near the galactic plane, and for them the frequency of surrounding external galaxies is a fair measure of the intervening space absorption in the cluster's direction.

New information on interstellar transparency is now available for much of the sky from the surveys of faint galaxies, and we can proceed to revise the distances of globular clusters that are not too near the galactic plane. For many of them we now have revised distance moduli, based on new photometry of the variables or the bright cluster stars from the David Dunlap, Harvard, Mount Wilson and other observatories. In the far southern sky, where many of the high-latitude clusters are found, the photographic magnitude system, for stars as faint as those in many of the globular clusters, is still provisional.

2. In table 1 we have assembled, chiefly from *Star Clusters*,[2] some descriptive data concerning the globular clusters for which revised values of the distances have now been determined. Galactic coördinates λ and β, refer to the pole at 12^h40^m, $+28°$ (1900). The angular diameters, except one in parentheses, are those microdensitometrically measured by Shapley and Sayer.[3] The integrated magnitudes are, when possible, taken from Christie's schraffiekassette work;[4] otherwise they are values determined from Harvard patrol plates and are reduced to the Christie scale.

3. The new results for the high-latitude globular clusters are collected in table 2. In the first section of the table are the objects for which the present results are the most dependable. The lower reliability for the clusters in the second section arises from various sources; in general, the observed quantities that contribute to the low weight are indicated by colons. The best one-half of the entries in the second section are marked by asterisks after the NGC number. A letter *n* refers to a note at the end of the table.

The third, fourth and fifth columns of table 2 give the results of the nebular counts on the best available long-exposure plates made with the Bruce and Metcalf telescopes for the southern and northern skies, respectively. The average number of galaxies per square degree, $\overline{N}$, generally refers to a surrounding or adjacent area of not less than nine square de-

TABLE 1

NGC	R. A. (1900)	DEC.	λ	β	DIAMETER	TOTAL PG. MAGNITUDE	NO. OF VARIABLES
104	0^{h}19^m.6	−72°38′	272°	−45°	53′.6	(4.5)	8*
288	0 47.8	−27 08	157	−88	13.1	8.96	2*
362	0 58.9	−71 23	268	−47	17.7	8.0	14
1261	3 9.5	−55 36	237	−51.5	...	9.5	0
1851	5 10.8	−40 09	212	−34.5	11.5	7.72	3*
2419	7 31.4	+39 06	148	+26	5.1	11.51	36
4147	12 5.0	+19 06	226	+79	2.8	11.01	4
4590	12 34.2	−26 12	269	+36	...	9.12	28
5024	13 8.0	+18 42	305	+79	15.8	8.68	40
5053	13 11.5	+18 13	310	+78	...	10.9	9
5272	13 37.6	+28 53	8	+78	22.1	7.21	185
5466	14 1.0	+29 00	8	+72.5	...	10.39	14
5634	14 24.4	− 5 32	310	+48.5	6.8	10.8	4*
5694	14 33.8	−26 36	299	+29	...	10.87:	0
5897	15 11.7	−20 39	312	+29	13.1	9.61	0
5904	15 13.5	+ 2 27	332	+46	25.0	7.04	97
6205	16 38.1	+36 39	27	+40	18.1	6.78	11
6218	16 42.0	− 1 46	344	+25	21.0	7.95	1
6229	16 44.2	+47 42	40	+40	5.3	10.26	21*
6254	16 51.9	− 3 57	343	+22	21.5	7.64	2
6341	17 14.1	+43 15	36	+35	(14)†	7.30	16
6752	19 2.0	−60 48	303	−26.5	41.9	7.2:	1*
6809	19 33.7	−31 10	336	−25	28.7	7.08	2*
6864	20 0.2	−22 12	347	−27	8.7	9.50	11*
6934	20 29.3	+ 7 04	20	−20	...	10.01	51*
6981	20 48.0	−12 55	3	−34	8.0	10.24	31
7006	20 56.8	+15 48	32	−21	...	11.45	20
7078	21 25.2	+11 44	33	−28	18.1	7.33	74
7089	21 28.3	− 1 16	21	−36	16.9	7.30	17
7492	23 3.1	−16 10	22	−64	...	12.33	9*

* Distances do not depend on variable stars.

† Diameter of NGC 6341 from Nassau, J. J., *Ap. J.*, **87**, 366 (1938).

grees. The magnitude limit to which the count of galaxies refers is m_n, and the absorption δm is computed from the relation

$$\delta m = m_n - 1.67 \log \overline{N} - 15.2$$

which is based on our earlier determinations[5] of the space-density parameter for the galactic caps, $\overline{m}_1 = 15.2$.

The number of Cepheid variable stars that have been recorded in each cluster is shown in the last column of table 1.[6] When it was not possible to use the variables directly in the determination of the distance modulus, the number is marked with an asterisk; the modulus has then been determined from the cluster's bright stars and the integrated magnitude and diameter, which is also the procedure when no variables at all are known. The adopted distance modulus in the sixth column of table 2 includes the

TABLE 2a

NGC	MESSIER	$\bar{N}$	m_n	δm	DIST. MOD.	DIST. KPC	$r \sin \beta$ KPC	$r \cos \beta$ KPC	ABS. MAG.
104	47 Tuc	n	n	+0.3	14.4	7.6	− 5.4	5.4	−10.2
288		85	18.4	0.0	15.8	14.5	−14.5	10.5	−6.8
362		n	n	+0.3	15.0	10.0	− 7.3	6.8	−7.3
2419		n	n	+0.5	18.75	56.2	+24.6	50.4	−7.7
4147		76n	17.5	−0.8:	16.5	20.0	+19.6	3.8	−5.5
4590	68	8	17.0	+0.3	15.65	13.5	+ 7.9	10.9	−6.8
5024	53	41	17.7	−0.2	16.53	20.2	+19.8	3.9	−7.8
5053		41	17.7	−0.2	16.2	17.4n	+17.0	3.6	−5.3
5272	3	32n	17.2	−0.5	15.43	12.2	+11.9	2.6	−8.2
5466		56n	17.5	−0.6:	16.16	17.0	+16.2	5.1	−5.8
5694		n	n	+0.4:	17.6	33.1	+16	29	−7.1:
5897		19	17.7	+0.4	15.7	13.8	+ 6.7	12.1	−6.5
5904	5	26	17.6	0.0	15.03	10.1n	+ 7.3	7.0	−8.0
6205	13	14	17.0	−0.1	14.88	9.5n	+ 6.1	7.3	−8.1
6218	12	8	17.3	+0.6	14.6	8.3	+ 3.5	7.5	−7.3
6254	10	8	17.3	+0.6	14.6	8.3	+ 3.1	7.7	−7.6
6341	92	34	17.4	−0.3	15.06	10.3	+ 5.9	8.4	−7.8
6981	72	12	17.7	+0.7	16.1	16.6	− 9.3	13.8	−6.6
7078	15	44	18.2	+0.3	15.3	11.5	− 5.4	10.2	−8.3
7089	2	33	17.8	+0.1	15.7	13.8	− 8.1	11.2	−8.5

TABLE 2b

NGC	MESSIER	$\bar{N}$	m_n	δm	DIST. MOD.	DIST. KPC	$r \sin \beta$ KPC	$r \cos \beta$ KPC	ABS. MAG.
1261		21	17.3	−0.1	16.7:	22	−17	14	−7.2
1851		68	17.7	−0.5	15.8:	14	− 8	12	−8.1
5634		16	17.2	0.0	17.5:	32	+24	21	−6.7
6229*		27n	17.1	−0.5:	17.4	30n	+19	23	−7.1
6752		17	18.0	+0.8	13.8:	5.8	− 2.6	5.2	−7.4:
6809*	55	3	16.9	+0.9	13.8	5.8	− 2.4	5.3	−7.7
6864	75	8	17.0:	+0.3:	18.1:	42	−19	37	−8.9:
6934*		24:	18.2	+0.7:	16.3	18	− 6	17	−7.0
7006*		19	17.9	+0.6	18.2:	44	−16	41	−7.3
7492*		33	18.2	+0.5	17.0	25.1	−23	11	−4.7

NGC 104. See twelfth paper of this series, these PROCEEDINGS **27**, 440–445 (1941), for discussion of distance and absorption.

362. Absorption assumed the same as for the Small Magellanic Cloud, which surrounds it.

2419. Adopted value of absorption from Baade's discussion in *Mt. Wilson Contr.*, No. 529 (1935). A Harvard plate suggests a larger value, but the revision awaits further study of the surrounding regions.

4147, 5272, 5466, 6229. Clusters lie in regions rich in groups of galaxies.

5053. By comparing the color-magnitude array for this cluster with those I derived for Messier 3, 13 and 68, Cuffey has estimated the distance as 16 ±2 kpc. *Ap. J.*, **98**, 49–53 (1943). This cluster and NGC 4147, 5466 and 7492 belong to the so-called "giant-poór" category, with low absolute magnitudes.

5694. Baade reports little or no absorption (*Pub. Ast. Soc. Pac.*, **46**, 52 (1934)); my provisional estimate is $\delta m = +0.8$ from Bruce plates.

5904. The revised distance is based on my earlier general photometry and on a new study of the variables by Oosterhoff at Leiden (letter, dated December 19, 1940).

6205. Distance of Messier 13 revised with assistance of H. B. Sawyer's work on four Cepheids. *Pub. David Dunlap Obs.*, **1**, 11 (1942).

6229. Distance can be precisely determined when the 20 new variables (unpublished), discovered by Baade at Mt. Wilson, are worked up.

correction for space absorption, column 5, and involves also whatever revision we have been able to make on the basis of recent photometric work at Harvard, Mount Wilson (Baade), Perkins (Nassau), David Dunlap (Sawyer), Babelsberg (Hachenberg), Leiden (Oosterhoff) and Bergedorf (Grosse) observatories.

No absorption correction has been applied when δm is negative. When it is positive and the latitude is greater than $\pm 40°$, also no correction has been made, except for the two clusters NGC 104 and 362 which are near the Small Magellanic Cloud and appear to suffer from its absorbing dust or from a flare of absorption extending from the Milky Way. The negative

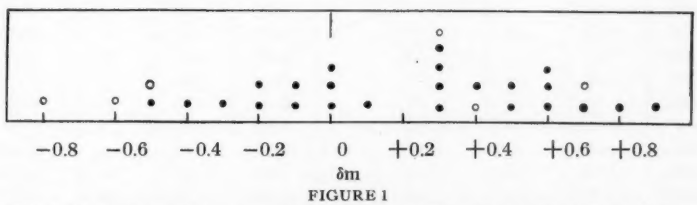

FIGURE 1

Distribution of absorption corrections. Low-weight values indicated by circles.

values of δm reflect chiefly the uneven distribution and in particular the excesses in the number of faint galaxies; we must, of course, expect that the positive values frequently reflect true deficiencies in number rather than space absorption. Figure 1 shows the distribution of δm.

The distances in the seventh to ninth columns of table 2 are "reduced to the galactic poles"; that is, they are calculated on the assumption that there is no absorption in the galactic polar caps—an assumption which implies that the Sun is located in an open space in the scattered and irregular clouds of absorption along the Milky Way plane. The components of the distance perpendicular to and in the galactic plane are given in the eighth and ninth columns, respectively; β is the galactic latitude.

As mentioned above, the evidence from the nebular distribution and from the colors of clusters and galaxies suggests that the assumption of polar-cap transparency cannot be far wrong. If there is an appreciable absorption at the galactic poles, all the distances in columns seven, eight and nine of table 2 should be multiplied by the following factors:

If total absorption at pole is	f =
0.1	0.955
0.2	0.91
0.3	0.87

Hubble has used 0.25 for the total photographic absorption at the galactic poles; Stebbins and Whitford, a somewhat smaller value.

If such a correction factor should be applied to the distances in table 2, it probably would be appropriate first to use all the positive and at least the smaller negative corrections for absorption, rather than follow the procedure described above. Such a plan would merely imply that we adopt a specific *average* space absorption for high galactic latitudes, but that here and there we find either excessive absorption and a positive δm, or clear spaces with consequent high nebular number and a negative absorption correction.

TABLE 3

COMPARISON OF REVISED DISTANCES WITH 1930 VALUES

NGC	GALACTIC LATITUDE	1930 VALUE KPC	RATIO	NGC	GALACTIC LATITUDE	1930 VALUE KPC	RATIO
104	−45°	6.8	1.12	6205	+40°	10.3	0.93
288	−88	14.5	1.00	6218	+25	11.0	0.75
362	−47	12.9	0.78	6229	+40	29.8	1.01
1261	−51.5	22.0	1.00	6254	+22	11.2	0.74
1851	−34.5	14.3	0.98	6341	+35	11.2	0.92
4147	+79	24.2	0.83	6752	−26.5	8.4	0.69
4590	+36	15.5	0.87	6809	−25	8.8	0.66
5024	+79	18.2	1.11	6864	−27	48.5	0.87
5053	+78	17.3	1.00	6934	−20	24.9	0.72
5272	+78	12.2	1.00	6981	−34	23.3	0.71
5466	+72.5	17.0	1.00	7006	−21	56.8	0.78
5634	+48.5	31.4	1.02	7078	−28	13.1	0.88
5897	+29	16.4	0.84	7089	−36	13.9	0.99
5904	+46	10.8	0.94	7492	−64	25.2	0.99

4. The new results for the distances are compared in table 3 with my original values, published on the currently-accepted zero point in 1930.[2] Naturally there is on the average little change for the objects in the higher latitudes; we have the mean ratio New/Old = 0.98 ± 0.03 (m. e.) for the twelve clusters with latitudes higher than 40°. The change is considerable, however, with latitudes from 20° to 40°, where for sixteen clusters we have, in the mean, New/Old = 0.83 ± 0.03 (m. e.). The corrections for space absorption produce most of the change.[7]

The distances from the galactic plane, $r \sin \beta$, in column 8 of table 2, show results now well known—namely, the great thickness of the Milky Way system, if we assume, as is natural, that most if not all the high-latitude globular clusters are members of the Galaxy. It is of interest to compare the largest values, around 20 kiloparsecs above and below the

galactic plane with the values $r \sin \beta$ for the Magellanic Clouds, 12 kiloparsecs (Large) and 18 kiloparsecs,[8] and for the faintest of the independent high-latitude cluster-type Cepheids, 10 to 15 kiloparsecs.[9]

5. In the final column of table 2 are the absolute photographic magnitudes of the thirty globular clusters. Their dispersion is shown in figure 2, which resembles a diagram given by Christie.[4]

The greatest of these globular clusters, 47 Tucanae, exceeds in total absolute brightness some of the dwarf irregular galaxies of the Magellanic type. The globular cluster Omega Centauri is of comparable absolute magnitude, but its low latitude, $\beta = +15°$, excludes it from the tabulations above. For it a revised photometry by Martin,[10] and an unpublished Harvard nebular survey that suggests an absorption of +0.5, would give it the distance of 6.8 kiloparsecs, the same as my 1930 value, and an absolute magnitude of −10.0.

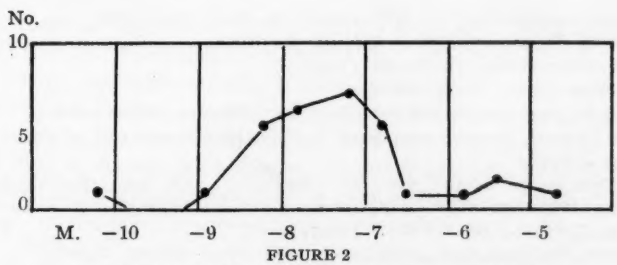

FIGURE 2

Thirty globular clusters. Spread of absolute magnitude.

6. *Conclusions and Summary.*—(*a*) The distances of thirty globular clusters in intermediate and high galactic latitudes have been revised on the basis of (1) recent investigations of the photographic magnitudes of bright stars and of Cepheid variables in the clusters, and (2) a census of the background of external galaxies, which gives evidence on the transparency of space between the observer and the clusters.

(*b*) The over-all diameter of the Milky Way in its plane is not well indicated by the revised distances, because of the necessary avoidance of low-latitude objects; but the earlier estimates of a distance to the center of approximately ten kiloparsecs are consistent with the new values of the distances of clusters.

(*c*) The over-all thickness of the system of globular clusters exceeds forty kiloparsecs. The weighted mean $r \sin \beta$ for the five clusters most distant from the galactic plane on the north side is +19.3 kiloparsecs, and for the five most distant on the south side, −17.5 kiloparsecs. The clusters apparently have a spatial distribution comparable with the haze of cluster-type Cepheids discussed in the first paper of this series.

(*d*) The integrated absolute magnitudes of the thirty globular clusters show a small dispersion around the mean value of −7.5 (photographic), except that the great globular cluster 47 Tucanae stands out as nearly three magnitudes brighter than the mean (as does Omega Centauri), and the "giant-poor" clusters, NGC 4147, 5053, 5466, 7492, are all fainter than the average, with values lying between −4.8 and −5.9. It is noteworthy that the absolute magnitudes of several of the dwarf galaxies of the local group of galaxies are between −9 and −12; and, of probably much higher significance in the hypothetical evolution of galaxies, the absolute magnitudes of the nuclei of the spirals NGC 598 (Messier 33) and 7793 are −8.0 and −7.3, respectively. The "escape" of the spiral arms and their background of stars, in a developmental trend from spiral to globular form,[11] would leave these two objects as globular clusters of average absolute luminosity.

[1] Stebbins and Whitford, *Mt. Wilson Contr.*, No. 547, p. 10 f (1936).

[2] *Harv. Obs. Monographs*, No. 2, Appendix A (1930).

[3] These PROCEEDINGS, **21**, 593–597 (1935).

[4] *Mt. Wilson Contr.*, No. 620 (1940).

[5] These PROCEEDINGS, **26**, 599–604 (1940), the tenth paper of this series.

[6] From Helen B. Sawyer's compilation in *Pub. David Dunlap Obs.*, **1**, No. 4 (1939), with some additions.

[7] Two clusters are omitted from the comparison: NGC 2419, the "intergalactic tramp," and NGC 5694 which was identified as a globular cluster after the earlier study: Lampland and Tombaugh, *Ast. Nach.*, **246**, 171 (1932).

[8] *Galaxies*, Blakiston, 1943, p. 51.

[9] These PROCEEDINGS, **25**, 423–428 (1939), the first paper of this series.

[10] *Leiden Obs. Ann.*, **17**, pt. 2, 1–166 (1938).

[11] *Galaxies*, Blakiston, 1943, p. 216.